Dynamical origin of anomalous temperature hardening of elastic modulus in vitreous silica

S. Ayrinhac,[1,2,3] B. Rufflé,[1,2] M. Foret,[1,2] H. Tran,[1,2] S. Clément,[1,2] R. Vialla,[1,2] R. Vacher,[1,2] J. C. Chervin,[3] P. Munsch,[3] and A. Polian[3]

[1]*Université Montpellier 2, Laboratoire Charles Coulomb UMR 5221, F-34095 Montpellier, France*

[2]*CNRS, Laboratoire Charles Coulomb UMR 5221, F-34095 Montpellier, France*

[3]*Institut de Minéralogie et de Physique des Milieux Condensés, Université Pierre et Marie Curie - Paris 6, CNRS UMR 7590, 4 place Jussieu, F-75252 Paris Cedex 05, France*

(Received 17 February 2011; revised manuscript received 5 May 2011; published 5 July 2011)

High-resolution Brillouin scattering experiments are performed under hydrostatic pressures ranging from 0 to 10 GPa in vitreous silica. The hypersound-attenuation coefficient exhibits a sharp maximum located at 2 GPa, which appears to coincide with the well-known minimum in sound velocity. Two main processes contribute to sound damping: the thermal relaxation of local defects and the anharmonic interactions with thermal vibrations. By analyzing the temperature dependence of the velocity and subtracting the changes produced by the above mechanisms, the unrelaxed velocity is found. It is constant at low temperatures and increases anomalously above a temperature onset. We show that the onset strongly depends on pressure, which is in agreement with a dynamical origin of the structural changes that produce the hardening.

DOI: 10.1103/PhysRevB.84.024201 PACS number(s): 64.70.kj, 78.35.+c, 62.50.−p, 62.40.+i

I. INTRODUCTION

Silica and silicates are among the most important components of Earth's mantle. Furthermore, in its vitreous state, silica is widely used in technological applications, such as telecommunication fibers. It is thus of crucial importance to understand the thermomechanical properties of silica, both in the molten and in the vitreous states. These properties are known to exhibit anomalous behaviors. In particular, the compressibility at room temperature increases first with pressure P in the range of 0 to about 2–3 GPa. Above 3 GPa, the compressibility decreases.[1,2] The associated change in density is fully reversible up to nearly 10 GPa. Above this value, a permanent densification occurs.[3–5] X-ray diffraction and Raman-scattering experiments have shown that the structure of the elementary units remains tetrahedral in the elastic domain, at between 0 and 10 GPa.[6,7] This was confirmed by numerical simulations.[8] For higher hydrostatic pressure, important changes in the network topology occur, producing irreversible densification. In the elastic domain, Huang and Kieffer[9] observed in numerical simulations that changes in the applied P induce local modifications of ring structure via 90° rotations of Si-O-Si bonds. This change in local structure is similar to that observed between the α and β phases of cristobalite. A similar behavior was also found in more recent simulations.[10] By noticing that α-cristobalite has a higher density and lower bulk modulus than the β phase, the compressibility anomaly is explained by a continuous change in ring configurations with P. Another explanation for the compressibility maximum is based on rigidity arguments.[11] This model assumes the existence of a distribution of floppy modes whose frequency changes with the applied pressure, with the network being most flexible at pressures around the compressibility maximum. In these pictures, the compressibility anomaly is dynamical in nature.

Anomalies also occur in the temperature dependence of the thermomechanical properties. At low-temperature T, the thermal expansion coefficient α of vitreous silica is negative, with a minimum near 50 K.[12] Also, with increasing T, the elastic moduli decrease to a frequency-dependent minimum in the range 20–60 K,[13] then they increase over a large T domain, up to the glass-transition temperature T_g.[14] Due to the very small value of α, the density is almost constant, and a similar extremum is also observed in the T dependence of the sound velocities v. The low-temperature decrease of $v(T)$ is explained by the coupling of acoustic waves with thermally activated relaxation (TAR) of structural elements,[15–17] whose nature is still unknown. This mechanism is also commonly accepted as the explanation for the well-known maximum observed in the sound attenuation in this temperature domain. In addition to this mechanism, variations of v with T are produced by anharmonic interactions of thermal vibrational modes. When these variations are subtracted from the experimental values, one might expect to obtain a constant bare velocity, the so-called unrelaxed velocity v_∞. In fact, at ambient pressure, the bare sound velocity is found to be constant from 0 to about 100 K, and then it increases almost linearly up to T_g.[18] We show in the present work that the onset of the anomalous $v_\infty(T)$ increase strongly depends on pressure, suggesting a dynamical origin for the temperature hardening of the elastic modulus in vitreous silica.

In Sec. II, we discuss the main available results for the P-T dependence of the sound attenuation and velocity in silica. Our experimental arrangement and our measurements are presented in Sec. III. Data analysis is described in Sec. IV and we discuss our findings in Sec. V. A summary is presented in Sec. VI.

II. SUMMARY OF RELEVANT RESULTS

Figure 1 shows the temperature dependence of ultrasonic attenuation measured for different applied pressures in the range 0–0.42 GPa.[19] The well-known maximum is observed, and seen to shift strongly to higher T with increasing P. These results can be fully accounted for on the basis of the phenomenological TAR model. In this model, structural defects are represented by particles relaxing in an asymmetric double-well potential. To account for the shape of $Q^{-1}(T)$,

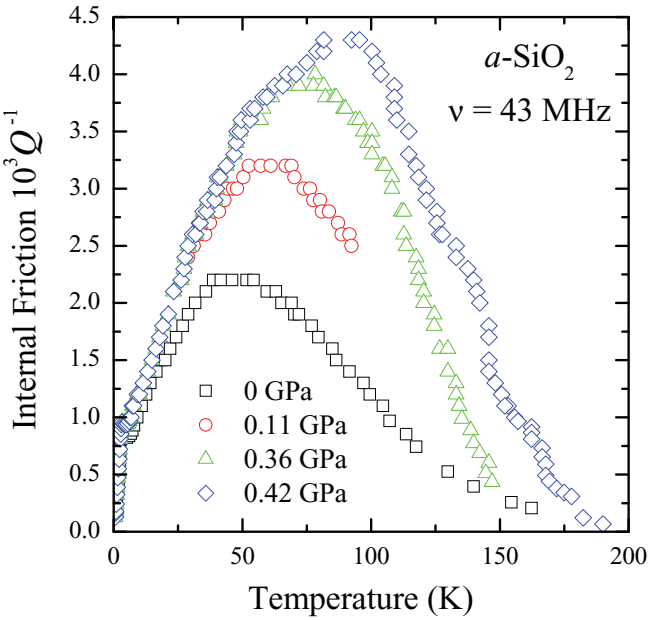

FIG. 1. (Color online) Internal friction for longitudinal modes, measured at 43 MHz in function of temperature and under several pressure values, from Ref. 19.

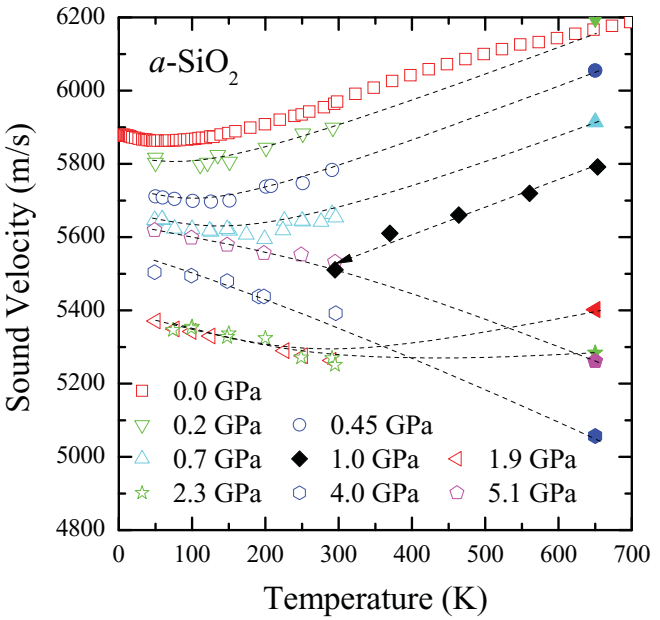

FIG. 2. (Color online) Sound velocity of longitudinal waves as a function of temperature at several pressure values. The open symbols arise from Brillouin scattering measurements at frequencies in the range 30–35 GHz (Refs. 20–22), while the solid symbols result from ultrasonic measurements at frequencies of a few tens of MHz (Refs. 23 and 24). The dashed lines are guides for the eyes.

a broad distribution must be assumed for both the potential asymmetry and the energy barriers. The shift observed for the maximum in $Q^{-1}(T)$ can be associated with an increase of barrier heights with increasing P. Another observation is that the amplitude of the peak in $Q^{-1}(T)$ is seen to increase with P. We will return to this point below.

Ultrasonic and Brillouin scattering measurements of the T dependence of v at different P from the literature are presented in Fig. 2. They cover the ranges from 0 to 5 GPa in P, and from 0 to 650 K in T. At room-temperature, $v(P)$ decreases first in the range 0–2 GPa, then increases above 3 GPa. Furthermore, for P values up to about 2 GPa, the minimum in $v(T)$ is seen to shift to higher T with increasing P. As already noted in Ref. 21, this minimum nearly coincides with the maximum in $Q^{-1}(T)$. Another point is that the hardening with T observed at ambient pressure remains in the measurements up to 1 GPa.

It was shown in Ref. 18 that in addition to the TAR mechanism, the strong effect of anharmonicity must be taken into account to explain the variations of both $v(T)$ and $Q^{-1}(T)$. This mechanism has been often ignored, as it hardly affects Q^{-1} at ultrasonic frequencies. The effect of anharmonicity on $v(T)$ becomes very important above 100 K, and thus it contributes to the shift of the minimum of $v(T)$ with increasing P, as can be observed in Fig. 2. In order to clarify the situation, we performed Brillouin scattering measurements of $v(P)$ and $Q^{-1}(P)$ and re-analyzed the previous results, including the combined effects of TAR and anharmonicity.

III. MEASUREMENT TECHNIQUES AND RESULTS

Brillouin scattering measurements were performed using a high-resolution Fabry-Pérot (FP) spectrometer described elsewhere.[25] In this tandem instrument, a four-pass plane FP is used as a monochromator to reduce the intensity of the elastic-scattering line. The resolving unit is a confocal spherical FP with a free spectral range of 3 GHz. The exciting radiation is the $\lambda_0 = 514.5$ nm line of a single-frequency argon-ion laser. Measurements were performed in backscattering. In order to take advantage of the high accuracy of the instrument, we have performed first a series of measurements at ambient pressure in the temperature range 5 to 700 K.

High-pressure measurements up to 6 GPa were performed in a Chervin-type diamond anvil cell (DAC) with culets of 800 μm diameter. The sample is Tetrasil SE fused silica ([OH] $\simeq$100 ppm) with 65 μm thickness. It is loaded in a chamber of 150 μm diameter drilled in a stainless-steel gasket. Hydrostatic compression is provided with a 4:1 methanol-ethanol mixture as the transmitting medium and calibrated with a ruby sphere.[26] The accuracy of pressure measurements is 0.1 GPa. For pressures above 6 GPa, we use a DAC with 400 μm culet diameter. The thickness of the sample is then 46 μm for measurements up to 8 GPa, and 24 μm above that.

A series of spectra recorded in the pressure range from 0 to 9.2 GPa is presented in Fig. 3. Each spectrum is obtained in about 1 hour, with a high signal-to-noise ratio. Comparing the profile of the elastic peak to that of the Brillouin line, it is evident that the linewidth can be extracted with excellent accuracy. For each spectrum, the position of the maximum of the Brillouin line is shown by an arrow. As expected, the Brillouin peak shifts to lower frequencies with increasing P up to 2 GPa. Simultaneously, a strong broadening is observed. Above 2 GPa, the peak moves to higher frequencies and narrows with increasing P.

The Brillouin spectra are fitted to a damped harmonic oscillator convoluted with the instrumental profile taken from the elastic line. The parasitic broadenings due to the large

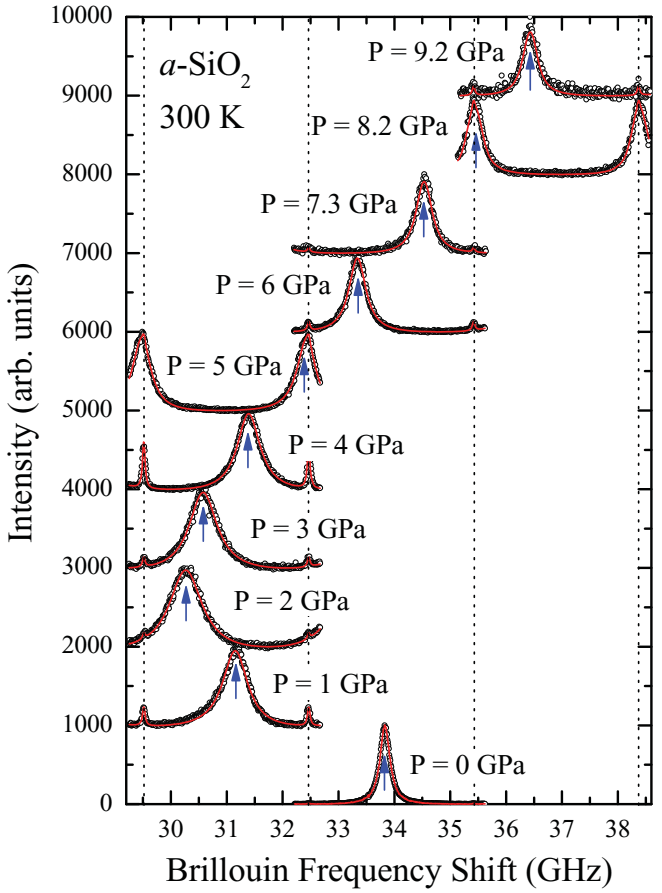

FIG. 3. (Color online) Typical spectra at hydrostatic pressures up to nearly 10 GPa. Three full orders of the spherical FP analyzer are shown. The four dashed lines indicate the elastic peaks periodically transmitted. The Stokes Brillouin peaks are indicated by the arrows. The solid red lines are fits explained in the text.

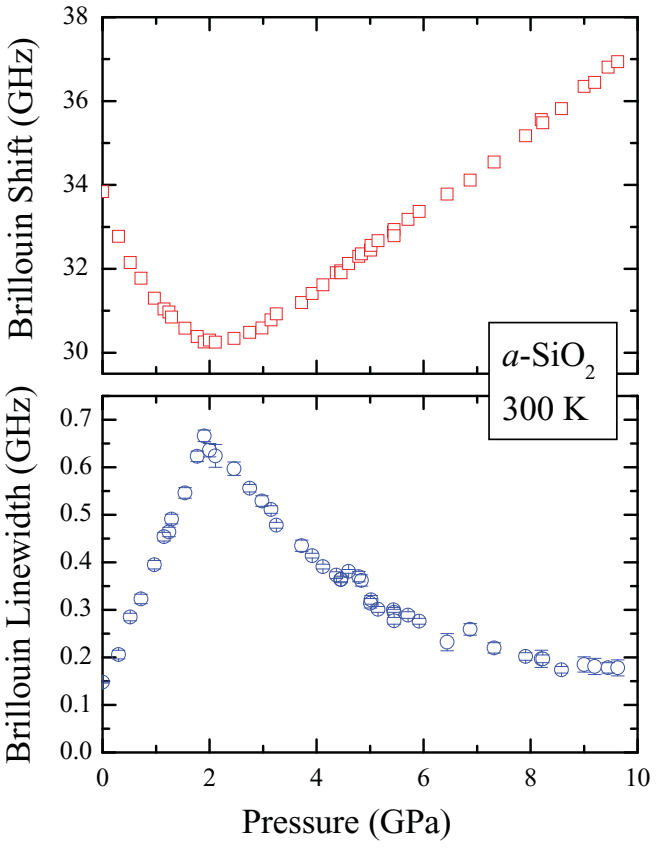

FIG. 4. (Color online) Brillouin frequency shift (top) and full width at half maximum (bottom) as a function of hydrostatic pressure at room temperature.

collection aperture ($\simeq$174 mrad) and to the finite size of the scattering volume are taken into account.[27] Care is taken to account for the change of length of the sample with applied P. The results for the Brillouin frequency shift $\delta\nu$ and full width at half maximum $\Gamma/2\pi$ are shown in Figs. 4(a) and 4(b), respectively. The results for the frequency shift are in excellent agreement with previous measurements in Refs. 28, 29, and 21. The high accuracy of the data allows one to locate precisely the minimum at 2.0 ± 0.1 GPa. An increase by a factor of about 4 in the Brillouin linewidth is observed from ambient pressure to $P = 2$ GPa. The peak in linewidth coincides almost exactly with the minimum in the frequency shift. At 10 GPa, the linewidth recovers nearly the value observed at normal pressure. The small accident observed in the curve around 4.5 GPa is an artifact due to overlapping of the Brillouin line of silica with that scattered by the pressure-transmitting alcohol. We have performed several cycles of compression and decompression. The results are found to be fully reversible when the maximum pressure remains below 9.5 GPa. In this P range, a constant value of the Brillouin frequency shift is observed when the sample is kept at the same P for a long time. In contrast, at larger applied pressure, a slow drift with time is observed, likely resulting from plastic events.[30] In the following, our analysis is limited to pressure in the range 0–5 GPa and temperature below 650 K, i.e., in the purely elastic regime.[31]

IV. DATA ANALYSIS

The main purpose of this paper is to analyze the temperature hardening in vitreous silica. For this purpose, it is essential to establish precisely the velocity changes $\delta v/v$ associated with the dissipative mechanisms. These changes can be calculated when the relevant parameters are obtained from an analysis of the internal friction. From the Brillouin frequency shift and linewidth, the sound velocity and internal friction are obtained as

$$v = \frac{\lambda_0 \delta\nu}{2n}, \tag{1}$$

where n is the refractive index taken from Refs. 32 and 29, and

$$Q^{-1} = \frac{\Gamma}{2\pi\delta\nu}. \tag{2}$$

As already discussed above, the internal friction at GHz frequencies probed by Brillouin scattering originates mainly from combined anharmonic losses and TAR.

We summarize here the method used in Ref. 18 to determine the effect of anharmonicity at ambient pressure on the basis of measurements of $v(\Omega,T)$ and $Q^{-1}(\Omega,T)$ over a broad frequency range. It is generally agreed that sonic and ultrasonic damping at temperatures above 10 K is dominated by thermally

activated relaxations. The phenomenological expression for the TAR losses is[20]

$$Q^{-1}_{\mathrm{TAR}}(\Omega,T) = \frac{\gamma^2}{\rho v^2 T}\int_{-\infty}^{\infty} d\Delta \int_0^{\infty} dV \times P(\Delta,V)\,\mathrm{sech}^2\frac{\Delta}{2T}\,\frac{\Omega\tau}{1+\Omega^2\tau^2}, \quad (3)$$

where Ω is the angular frequency, ρ is the density, v is the sound velocity, and T is the temperature in energy units. Δ and V are the parameters characterizing the double-well potentials, asymmetry and barrier height, respectively. $P(\Delta,V)\,d\Delta\,dV$ is the density of double-well entities. $\gamma = \frac{1}{2}\partial\Delta/\partial e$ is a deformation potential. In this equation, τ is the relaxation time for hopping within the double-well:

$$\tau = \tau_0 \exp\frac{V}{T}\,\mathrm{sech}\frac{\Delta}{2T}, \quad (4)$$

where τ_0 is the inverse of an attempt frequency (see, e.g., Ref. 17). In the fitting procedure, described in detail in Ref. 18, it is assumed that the distribution $P(\Delta,V)$ is the product of two single-variable distribution functions, i.e., a Gaussian in Δ, $f(\Delta) \propto \exp(-\Delta^2/2\Delta_C^2)$ of width Δ_C, times a modified Gaussian $g(V) \propto (V/V_0)^{-1/4}\exp(-V^2/2V_0^2)$ of width V_0.[33] By fitting ultrasonic results over a broad frequency range, the relevant parameters V_0, Δ_C, and τ_0 are extracted. From theses parameters, the TAR contribution at Brillouin scattering frequencies is calculated. Subtracting this contribution from the experimental data, a residual internal friction is finally obtained. These losses originate from anharmonic interactions between collective thermal motions of atoms. A detailed analysis of this mechanism was done by Maris in Ref. 34 for anharmonic interactions in crystals. In the Boltzmann equation framework, phonons are treated as a gas in which interactions lead to a mean thermal time $\tau_{\mathrm{th}}(T)$ between collisions.[34,35] The same approach can be used for glasses. This was done in particular by numerical simulation in the case of amorphous silicon.[36] The internal friction is given by

$$Q^{-1}_{\mathrm{anh}}(\Omega,T) = A\Omega\tau_{\mathrm{th}}/\left(1+\Omega^2\tau_{\mathrm{th}}^2\right), \quad (5)$$

with

$$A = \frac{C_{\mathrm{v}} T v}{2\rho v_{\mathrm{D}}^3}\bar{\gamma_{\mathrm{G}}}^2. \quad (6)$$

Here, C_{v} is the specific heat per unit volume, v_{D} is the Debye velocity, and $\bar{\gamma_{\mathrm{G}}}$ is an average Grüneisen constant, describing the change in frequency of the thermally excited modes under the strain imposed by the acoustic wave.

A similar analysis is followed in the present work. The temperature dependence of Q^{-1} measured in Brillouin scattering at four different P is shown in Fig. 5. The anharmonic contribution to $Q^{-1}(T)$ evaluated at ambient pressure in Ref. 18 is plotted as a dotted line in Fig. 5(a). Numerical simulations show that the vibrational density of states is almost constant for $P \leqslant 10$ GPa in the frequency range where modes are populated at room-temperature and below.[37] Therefore C_v and τ_{th} must hardly change with P in this pressure range. Moreover, the variations with P of ρ and v are also small in this P domain. We thus keep the same values for the anharmonic contribution to internal friction over the whole P range [see dotted lines in Figs. 5(b)–5(d)]. After

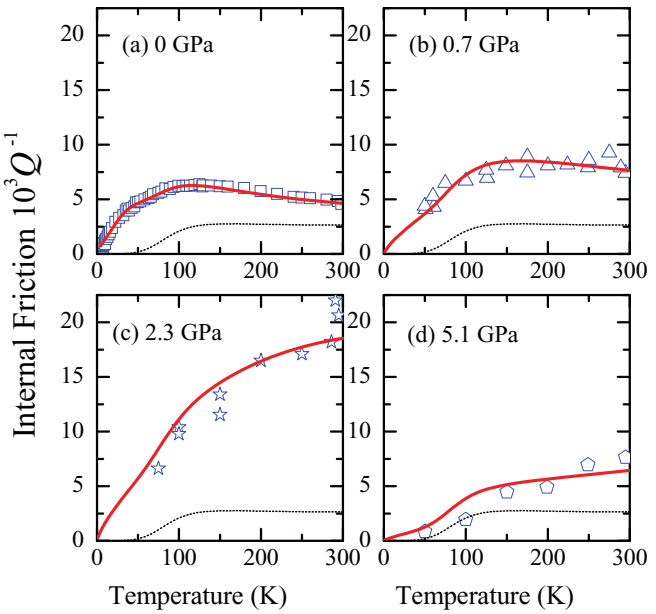

FIG. 5. (Color online) The internal friction in function of temperature at (a) ambient pressure (this work), and (b)–(d) 0.7, 2.3, and 5.1 GPa from Refs. 20 and 21. The dotted lines are the P-independent anharmonic contribution $Q^{-1}_{\mathrm{anh}}(T)$. The red solid lines are the entire adjustment described in the text, which is the sum of two contributions, $Q^{-1}_{\mathrm{anh}}(T)$ and $Q^{-1}_{\mathrm{TAR}}(T,P)$.

subtracting anharmonic losses from the experimental $Q^{-1}(T)$, the remaining contribution is fitted to Eq. (3). We simply assume a linear variation of the barrier-height distribution with pressure, keeping a constant cutoff V_{max} and an asymmetry width fixed to its ambient pressure value, $V_0/\Delta_C = 8.2$. We find $V_0(P) = 659 + 1265P$ with the cutoff value fixed to $V_{\mathrm{max}} = 1150$ K. The amplitude of the calculated curves is the second free parameter extracted from the fit. The solid lines in Fig. 5 are the sum of the anharmonic and TAR contributions. The agreement is excellent for $P = 0$ and $P = 0.7$ GPa. Above this, as the maximum is pushed beyond 300 K, the evaluation becomes more delicate. However, a fair adjustment is obtained. The same set of parameters also describes the Q^{-1} results in Fig. 1 at ultrasonic frequencies where the TAR mechanism is dominant. In particular, the changes in amplitude and peak position in $Q^{-1}(T)$ at various P are rather well reproduced.

V. DISCUSSION

Our $Q^{-1}(P)$ measurements at room-temperature are plotted in Fig. 6. The crosses result from the fits described above. The experimental profile is rather well reproduced. However, the amplitude of the measured curve is a little higher than that extracted from the fit, suggesting that the experimental values in Figs. 5(b)–5(d) could be underestimated. This might call for new accurate measurements under applied P as a function of T.

The product $\gamma^2 N_{\mathrm{TAR}}$ is obtained from the amplitude values extracted from the fits, with N_{TAR} being the total density of relaxing defects,

$$N_{\mathrm{TAR}} \equiv \int_{-\infty}^{\infty} d\Delta \int_0^{\infty} dV\, P(\Delta,V). \quad (7)$$

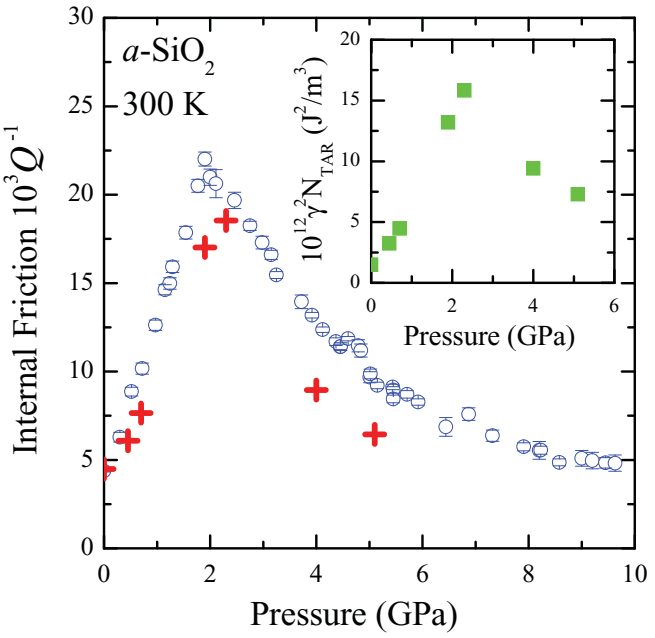

FIG. 6. (Color online) The internal friction as a function of pressure at room-temperature. Blue circles arise from our Brillouin scattering data, while red crosses are the room-temperature calculated values shown in Fig. 5. Inset: Pressure dependence of $\gamma^2 N_{\mathrm{TAR}}$ extracted from the fits (see text).

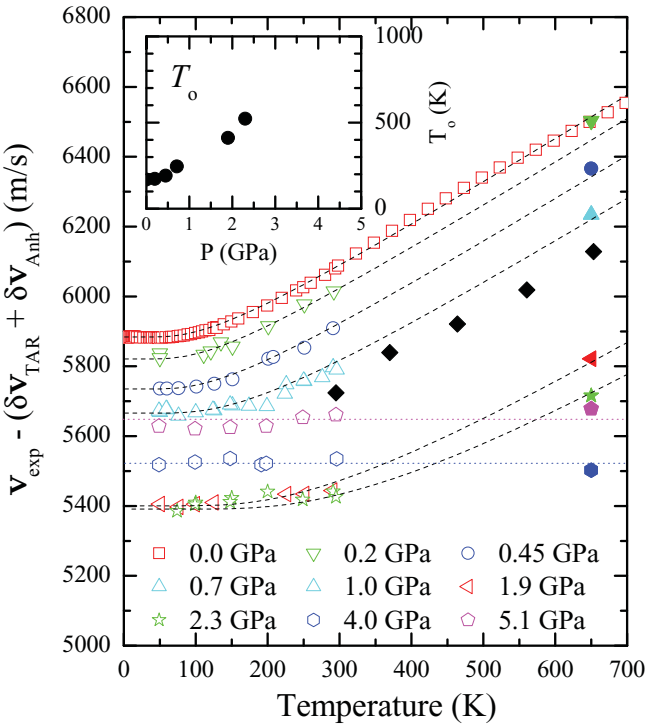

FIG. 7. (Color online) Temperature dependence of the calculated bare sound velocities at several pressure values. Symbols are identical to the ones used in Fig. 2. The dashed lines show our adjustment to a Wachtman law to extract the onset temperature T_o as explained in the text. The dotted lines are guides for the eyes, illustrating that T_o is pushed up beyond 650 K for pressure $\geqslant$4 GPa. Inset: Pressure dependence of T_o.

The values are shown in the inset of Fig. 6. It shows a pronounced maximum around 2 GPa. If the strong increase in $\gamma^2 N_{\mathrm{TAR}}$ from 0 to 2 GPa was related to N_{TAR}, it would imply an increase by one order of magnitude of the number of relaxing defects. Rather we suggest that the increase of the compressibility with P in this range produces an enhancement of the deformation potential. In this picture, the decrease of the compressibility beyond 2 GPa could also explain the maximum of $\gamma^2 N_{\mathrm{TAR}}$. Another explanation might be that the number of defects decreases at large P. This could be linked with the almost complete disappearance of TAR defects already observed in permanently densified silica glass upon 20% densification.[25,38]

We now turn to the temperature dependence of v. The variation $\delta v_{\mathrm{anh}}(T)$ at ambient pressure was calculated in Ref. 18. As done above for $Q^{-1}_{\mathrm{anh}}(T)$, we assume that this variation does not change with P. On the other hand, the TAR contribution $\delta v_{\mathrm{TAR}}(T)$ can be calculated using Eq. (1b) of Ref. 18 with the parameters obtained here from the evaluation of $Q^{-1}(T)$ at various P. The quantity $\delta v_{\mathrm{TAR}}(T) + \delta v_{\mathrm{anh}}(T)$ is then subtracted from the experimental data to obtain the bare velocities $v_\infty(T)$ at different P. The results are shown in Fig. 7 as open symbols for Brillouin scattering data and full symbols for ultrasonic measurements. It should be noted that by definition these bare velocities should not depend on the frequency of the measurement from which they are extracted. This makes it easier to compare results obtained by different techniques.

The most striking differences between the measured sound velocities $v(T)$ shown in Fig. 2 and the calculated $v_\infty(T)$ in Fig. 7 are that (i) the minimum observed in the former disappears completely in $v_\infty(T)$ and (ii) the negative slopes observed in $v(T)$ are removed in $v_\infty(T)$. Let us first consider the Brillouin scattering measurements. At 0, 0.2, 0.45, and 0.7 GPa, the bare velocity is constant at low T, then increases linearly above an onset temperature T_o. T_o is defined as the crossover temperature between the constant value at low T and the linear T dependence at high T, obtained from a Wachtman fit[39] to the data shown by the dashed lines in Fig. 7.[40] At larger P, the bare velocity obtained from Brillouin scattering measurements is nearly T independent. If we consider now the ultrasonic results at 1 GPa, we observe a linear increase above 300 K. Associating Brillouin and ultrasonic results for 1.9 and 2.3 GPa, we observe an increase of $v_\infty(T)$ at high temperature. The two lower dashed lines in Fig. 7 are the Wachtman fits to these data. At larger P, the measurements indicate that $v_\infty(T)$ is almost independent of T, suggesting that the onset temperature T_o may be above 650 K, out of the elastic domain. The values obtained for T_o are plotted in the inset of Fig. 7. T_o increases with P in the interval where we could determine it, from 170 K at 0 GPa to 500 K at 2.3 GPa. The results in Fig. 7 also indicate that it shifts much above room-temperature at larger P.

The variation of T_o with P can be explained by assuming that the applied pressure enhances the barrier heights between the two positions of structural units in a double-well potential. The activation energy is multiplied by almost 3 when P increases from 0 to 2.3 GPa. Another observation is that the slope of $v_\infty(T)$ is the same for $P = 0$ and $P = 1$ GPa. In the

above picture, this might indicate that the distribution of the barrier heights is not modified by the applied pressure. In the framework of the model presented in Ref. 9, the linear increase with T of elastic moduli is related to a change in the ring configurations via Si-O-Si bond rotations similar to the ones underlying the α-to-β cristobalite phase transformation.[41] In this picture, T_o marks the onset of these rotations, with the thermal energy becoming equal to the lowest energy barrier of the distribution. On the other hand, it would be interesting to know the temperature dependence of the bare velocity $v_\infty(T)$ predicted in the framework of the floppy modes model.[42]

VI. SUMMARY

We have performed accurate Brillouin scattering measurements of the velocity and attenuation of hypersonic waves as a function of pressure at room-temperature in vitreous silica. The results were analyzed together with previous literature data. Internal friction measurements are described satisfactorily using a model including dissipative effects of anharmonicity and thermally activated relaxation of structural defects. From this model, the associated velocity changes were calculated and then subtracted from the data to obtain the bare velocities as a function of T at different P. $v_\infty(T)$ is almost constant at low T, then increases linearly above a temperature onset T_o. We find evidence for an increase of T_o with P. This is in agreement with a dynamical origin of the structural changes which produce the temperature hardening of the elastic modulus in vitreous silica.

ACKNOWLEDGMENTS

We thank Professor E. Courtens for fruitful discussions and a careful critical reading of the manuscript. We also acknowledge the financial support of the Agence Nationale pour la Recherche (Grant No. ANR-05-BLAN-0367-04, *PlastiGlass*).

[1] P. W. Bridgman and I. Šimon, J. Appl. Phys. **24**, 405 (1953).
[2] J. Schroeder, T. G. Bilodeau, and X.-S. Zhao, High Press. Res. **4**, 531 (1990).
[3] M. Grimsditch, Phys. Rev. Lett. **52**, 2379 (1984).
[4] C. Meade and R. Jeanloz, Phys. Rev. B **35**, 236 (1987).
[5] A. Polian and M. Grimsditch, Phys. Rev. B **41**, 6086 (1990).
[6] C. Meade, R. J. Hemley, and H. K. Mao, Phys. Rev. Lett. **69**, 1387 (1992).
[7] Y. Inamura, Y. Katayama, .W. Utsumi, and K.-i. Funakoshi, Phys. Rev. Lett. **93**, 015501 (2004).
[8] R. G. Della Valle and E. Venuti, Phys. Rev. B **54**, 3809 (1996).
[9] L. Huang and J. Kieffer, Phys. Rev. B **69**, 224203 (2004).
[10] Y. Liang, C. R. Miranda, and S. Scandolo, Phys. Rev. B **75**, 024205 (2007).
[11] A. M. Walker, L. A. Sullivan, K. Trachenko, R. P. Bruin, T. O. H. White, M. T. Dove, R. P. Tyer, I. T. Todorov, and S. A. Wells, J. Phys. Condens. Matter **19**, 275210 (2007).
[12] G. K. White, Phys. Rev. Lett. **34**, 204 (1975).
[13] J. T. Krause and C. R. Kurkjian, J. Am. Ceram. Soc. **51**, 226 (1968).
[14] A. Polian, D. Vo-Tanh, and P. Richet, Europhys. Lett. **57**, 375 (2002).
[15] O. Anderson and H. Bömmel, J. Am. Ceram. Soc. **38**, 125 (1955).
[16] J. Jäckle, L. Piché, W. Arnold, and S. Hunklinger, J. Non-Cryst. Solids **20**, 365 (1976).
[17] K. S. Gilroy and W. A. Phillips, Philos. Mag. **43**, 735 (1981).
[18] R. Vacher, E. Courtens, and M. Foret, Phys. Rev. B **72**, 214205 (2005).
[19] U. Bartell and S. Hunklinger, J. Phys. (Paris) **43**, 489 (1982).
[20] S. Rau, S. Baethler, G. Kasper, G. Weiss, and S. Hunlinger, Ann. Phys. (Berlin) **4**, 91 (1995).
[21] D. Tielbürger, R. Merz, R. Ehrenfels, and S. Hunklinger, Phys. Rev. B **45**, 2750 (1992).
[22] B. Rufflé, S. Ayrinhac, E. Courtens, R. Vacher, M. Foret, A. Wischnewski, and U. Buchenau, Phys. Rev. Lett. **104**, 067402 (2010).
[23] H. Sato, K. Ito, and Y. Aizawa, Meas. Sci. Technol. **15**, 1787 (2004).
[24] A. Yokoyama, M. Matsui, Y. Higo, Y. Kono, T. Irifune, and K. Funakoshi, J. Appl. Phys. **107**, 123530 (2010).
[25] E. Rat, M. Foret, G. Massiera, R. Vialla, M. Arai, R. Vacher, and E. Courtens, Phys. Rev. B **72**, 214204 (2005).
[26] J.-C. Chervin, B. Canny, and M. Mancinelli, High Press. Res. **21**, 305 (2001).
[27] R. Vacher, S. Ayrinhac, M. Foret, B. Rufflé, and E. Courtens, Phys. Rev. B **74**, 012203 (2006).
[28] M. Grimsditch, Phys. Rev. B **34**, 4372 (1986).
[29] C.-S. Zha, R. J. Hemley, H.-K. Mao, T. S. Duffy, and C. Meade, Phys. Rev. B **50**, 13105 (1994).
[30] O. B. Tsiok, V. V. Brazhkin, A. G. Lyapin, and L. G. Khvostantsev, Phys. Rev. Lett. **80**, 999 (1998).
[31] F. S. El'kin, V. V. Brazhkin, L. G. Khvostantsev, O. B. Tsiok, and A. G. Lyapin, JETP Lett. **75**, 342 (2002).
[32] C. Z. Tan, J. Non-Cryst. Solids **238**, 30 (1998).
[33] R. Keil, G. Kasper, and S. Hunklinger, J. Non-Cryst. Solids **164–166**, 1183 (1993).
[34] H. J. Maris, in *Physical Acoustics*, edited by W. P. Mason and R. N. Thurston (Academic, New York, 1971), Vol. 8, pp. 279–345.
[35] V. Gurevich, in *Transport in Phonon Systems*, edited by V. Agranovich and A. Maradudin, Modern Problems in Condensed Matter Sciences (North-Holland, Amsterdam, 1986), Vol. 18.
[36] J. Fabian and P. B. Allen, Phys. Rev. Lett. **82**, 1478 (1999).
[37] M. Matsubara, S. Ispas, and W. Kob (unpublished).
[38] G. Weiss, A. Daum, M. Sohn, and J. Arndt, Physica B **219–220**, 290 (1996).
[39] J. B. Wachtman, W. E. Tefft, D. G. Lam, and C. S. Apstein, Phys. Rev. **122**, 1754 (1961).
[40] The results in Fig. 7 show that the slope of $v_\infty(T)$ between 300 and 700 K is the same for ambient pressure and for 1 GPa. Then the high-temperature limit for the slope is kept constant in the Wachtman fit.
[41] L. Huang and J. Kieffer, Phys. Rev. Lett. **95**, 215901 (2005).
[42] K. Trachenko, M. T. Dove, M. J. Harris, and V. Heine, J. Phys. Condens. Matter **12**, 8041 (2000).